Injectable hydrogel with nucleus pulposus-matched viscoelastic property prevents intervertebral disc degeneration

Haoruo Jia [a,1], Xiao Lin [b,1], Dong Wang [a], Jingwei Wang [c], Qiliang Shang [a], Xin He [c,d], Kang Wu [b], Boyan Zhao [e], Pandi Peng [f], Han Wang [a], Di Wang [a], Pan Li [a,g], Liu Yang [a,g], Zhuojing Luo [a,g,*], Lei Yang [b,h,**]

[a] Institute of Orthopedic Surgery, The First Affiliated Hospital, Fourth Military Medical University, Xi'an, 710032, China
[b] Orthopedic Institute and Department of Orthopedics, The First Affiliated Hospital, Soochow University, Suzhou, 215000, China
[c] Department of Medicine Chemistry and Pharmaceutical Analysis, School of Pharmacy, Fourth Military Medical University, Xi'an, 710032, China
[d] Air Force Hospital of Eastern Theater Command, Nanjing, 210000, China
[e] Department of Neurosurgery, The First Affiliated Hospital, Fourth Military Medical University, Xi'an, 710032, China
[f] Institute of Flexible Electronics, Northwestern Polytechnical University, Xi'an, 710129, China
[g] Medical Research Institute, Northwestern Polytechnical University, Xi'an, 710032, China
[h] Center for Health Science and Engineering (CHSE), School of Health Sciences and Biomedical Engineering, Hebei University of Technology, Tianjin, 300130, China

ARTICLE INFO

ABSTRACT

Background/Objective: Intervertebral disc (IVD) degeneration (IVDD) that greatly affected by regional biomechanical environment is a major cause of low back pain. Injectable hydrogels have been commonly studied for treatment of IVDD due to their capability of mimicking extracellular matrix structure to support cellular behavior and clinical prospects in minimally invasive treatment. However, most hydrogels suffer from complicated chemistry, potential uncertainty and toxicity from in-situ gelation, and mismatch with IVD mechanical environment that limit their therapeutic effects or clinical translation in IVDD or intervertebral disc defect repair. For IVD lesion repair, the study aims to develop a novel hydrogel with shear-thinning enabled injectability, high biosafety, and mechanical properties adaptable to the IVD environment, using a simple chemistry and method. And therapeutic efficacy of the novel hydrogel in the treatment of IVDD or intervertebral disc defect will be revealed.
Methods: A glycerol cross-linked PVA gel (GPG) was synthesized based on multiple H-bonds formation between glycerol molecules and PVA chains. The rheological and mechanical properties were tested. The swelling ratio was measured. The micro-architecture was observed through scanning and transmission electron microscopes. Nucleus pulposus (NP) cells were cultured in GPG-coated plates or silicone chambers treated under hydrostatic or dynamic loading in vitro, and examined for proliferation, vitality, apoptosis, expression of catabolic and anabolic markers. GPG was injected in needle puncture (IDD) or NP discectomy (NPD) models in vivo, and examined through magnetic resonance imaging, micro-computed tomography scanning and histological staining.
Results: GPG had a highly porous structure consisting of interconnected pores. Meanwhile, the GPG had NP-like viscoelastic property, and was able to withstand the cyclic deformation while exhibiting a prominent energy-dissipating capability. In vitro cell tests demonstrated that, the hydrogel significantly down-regulated the expression of catabolic markers, maintained the level of anabolic markers, preserved cell proliferation and vitality, reduced apoptotic rate of NP cells under pathologically hydrostatic and dynamic loading environments compared to cells cultured on untreated plate or silicone chamber. In vivo animal studies revealed that injection of GPG efficiently maintained NP structural integrity, IVD height and relative water content in IDD models, and stimulated the fibrous repair in NPD models.

* Corresponding author. Institute of Orthopedic Surgery, The First Affiliated Hospital, Fourth Military Medical University, Xi'an, 710032, China
** Corresponding author. Center for Health Science and Engineering (CHSE), School of Health Sciences and Biomedical Engineering, Hebei University of Technology, Tianjin, 300130, China.
E-mail addresses: haoruoj@163.com (H. Jia), xlin@suda.edu.cn (X. Lin), wangdongfmmu@hotmail.com (D. Wang), jingwei1010@qq.com (J. Wang), boishang@sina.com (Q. Shang), 1543618464@qq.com (X. He), 20194209298@stu.suda.edu.cn (K. Wu), zhao.boyan@hotmail.com (B. Zhao), pengpandi0@163.com (P. Peng), wh.23@hotmail.com (H. Wang), dr.wangdi@qq.com (D. Wang), lz02@mail.nwpu.edu.cn (P. Li), yangliu@fmmu.edu.cn (L. Yang), zjluo@fmmu.edu.cn (Z. Luo), ylei@hebut.edu.cn (L. Yang).
[1] H.J. and X.L. contributed equally to this work.

Conclusion: This study showed that GPG, with high injectability, NP-like viscoelastic characteristics, good energy-dissipating properties and swelling capacities, preserved NP cells vitality against pathological loading, and had therapeutic effects on IVD repair in IDD and NPD models.

The translational potential of this article: Effective clinical strategy for treatment of intervertebral disc degeneration (IVDD) is still lacking. This study demonstrates that injection of a hydrogel with nucleus pulposus-matched viscoelastic property could remarkably prevent the IVDD progress. Prepared with simple chemistry and procedure, the cell/drug-free GPG with high bio-safety and shear-thinning enabled injectability bears great translational potential for the clinical treatment of IVDD via a minimally invasive approach.

1. Introduction

Low back pain (LBP) as an extremely common musculoskeletal symptom in all age groups, leads to low life quality, productivity loss and high socioeconomic burden globally [1]. Recent studies identified intervertebral disc (IVD) degeneration (IVDD) as a major cause of LBP [2]. The elements of IVD, including nucleus pulposus (NP), annulus fibrosus (AF) and cartilage endplate (CEP), are all prone to different stresses, and each of these alone or in combination, can contribute to IVDD [3].

Sagittal spine balance and anatomic curvature influence the stability and integrity of IVD, while excessive mechanical stimuli can induce radial fissures accompanied by internal disruption of the AF and NP herniation [4]. Recent studies have elucidated that NP tissue, exerting a hydrostatic pressure which is mainly responsible for loading distribution by creating tension near its interface with AF, plays essential roles in maintaining the structure, function, extracellular matrix (ECM) homeostasis and mechanical properties to prevent IVDD while confronting pathological loading or diverse deformations [5]. However, this transfer mechanism is altered in degenerated discs. Remodeling of NP with significant decrease of water content leads to alterations of its mechanical properties, the formation of cracks and fissures in the AF arised from abnormal and repeated mechanical loading, thereby, provides the path for NP cells migration from the center toward the periphery and finally induces symptomatic LBP [6].

Prevention and treatment of LBP have been recognized as a pivotal challenge for all ages of people. To a large extent, therapy mainly begins with personal training and non-surgical treatment such as pharmacotherapy in combination with physical therapies and psychological treatments depending on pain classification. Operative methods (eg. decompression for neuropathic pain, disc replacement, and fusion for mechanical causes) will be taken into consideration when all other approaches fail to release pain or motion limitation [7]. Unfortunately, all interventions addressing only single, solitary cause, have their limited capacity [8]. Most nonsurgical therapies have limited effect in long-term pain-relieving, on other hand, surgical interventions usually resolve the pain and dysfunction of disc herniation and spinal stenosis more rapidly but surgical benefit wanes over time. Since most surgeries change original structural integrity, tissue homeostasis or mechanical properties of spine thereby arise postoperative complications such as IVDD, NP defect or adjacent segment disease [9]. Discectomy, for instance, relieves clinical symptoms efficiently but does not address the underlying diseases, thereby, leads to defect and unbalance of the NP [10]. Rigid implants used to avoid rehernation post-discectomy show effectiveness over short period while do not promote tissue healing and thus are unable to prevent IVDD in long-term clinical trials [11].

Recent studies demonstrated the enormous potential of biomaterials and tissue engineering strategies to totally or partially replace tissues or organs [12]. The choice of polymer is crucial in this regard as it should possess a high degree of modifiability for the specific application of interest [13]. Hydrogels consisting of hydrophilic polymers, are increasingly becoming important tools in tissue engineering due to its biocompatibility, tunable mechanical properties, and biodegradability [14]. Owing to the lack of blood vessel and poor migration ability, the self-healing ability of damaged NP is limited. Hydrogels bring a new therapeutic strategy for the restoration and regeneration of NP [15]. The advantages of reported hydrogels include rarely causing immune reactions, controllable degradation rate, nontoxic degradation products or final metabolites during in vivo applications [16]. However, injectable hydrogels for IVDD treatment are usually prepared with complicated chemistry/method and using ECM derived natural biomaterials to enhance bioactivity. Meanwhile, most of injectable hydrogels for IVDD repair undergo crosslinking in vivo from a pre-gel, which has the problem of unpredictable in vivo crosslinking (physical or chemical changes of hydrogel). Meanwhile, the gelation of many hydrogels requires the use of photocrosslinking or the addition of toxic cross-linking agents to induce gelation in vivo which can result in toxicity to the local tissues during delivery or after implantation due to insufficient gelling reactions. Importantly, hydrogels for IVDD treatment should adapt to IVD mechanical environment, which is rarely considered in previous studies. Therefore, the present study aimed to develop a novel hydrogel with shear-thinning enabled injectability, high bio-safety, and mechanical properties adaptable to the IVD environment using a simple chemistry and method, and reveal its potential in treatment of IVDD.

Poly (vinyl alcohol) (PVA) is a semi-crystalline material in nature, and can form non-toxic and mechanically strong hydrogels via hydrogen bond (H-bond) mediated crosslinking [17]. Glycerol, which has plenty of hydroxyl groups, can form multiple H-bonds with PVA and function as bridge molecules to connect PVA chains into 3D networks, thereby, enhance mechanical strength of the hydrogel [18]. Therefore, a novel injectable hydrogel is developed based on the glycerol-mediated crosslinking of PVA chains, and is optimized with NP-like biomimetic structure and viscoelastic properties to support the survival and functions of NP cells, and to maintain the biological and structural integrity of IVD by absorbing and transferring load. The glycerol cross-linked PVA hydrogel (GPG) demonstrated protective effects on the NP vitality against pathologically mechanical loading in vitro. Importantly, with needle puncture or NP discectomy animal models, the therapeutic effect of GPG on both IVDD and NP defect was verified after injected in IVD (Scheme 1).

2. Materials and methods

2.1. Preparation of GPG

1.2g PVA (polymerization degree 1750, Sinopharm Chemical Reagent Co, Ltd., Shanghai, China) was dissolved in 18.8 mL deionized water at 95 °C under stirring to prepare PVA solution. Subsequently, 28.2 mL glycerol (reagent grade, 99%, Vetec™) was slowly added into the PVA solution and stirred for 1 h at 95 °C to obtain a homogeneous viscous solution. The viscous PVA/glycerol solution was transferred into various molds for different characterizations. GPG was obtained after curing the PVA/glycerol solution at ambient environment for 24 h.

2.2. Rheological test

The rheological properties of the gel samples (20 mm in diameter and 1 mm thick) were measured using a rheometer (AR2000, TA Instruments, USA) [19]. Frequency sweep tests were performed from 0.1 Hz to 10 Hz at 37 °C and 1% strain. Three important parameters were determined: storage modulus (G'), loss modulus (G''), and loss factor (tan δ = G''/G').

2.3. Compression test

The compression tests were performed on gel samples (11.2 mm in diameter and 15 mm in height) by a universal mechanical tester (HY-0580, Shanghai Hengyi Co., Ltd., China) at a speed of 10 mm/min. For static compression test, the gel sample was compressed to fracture. The compressive modulus of each sample was determined from the slope of the stress–strain curve at a strain of 10%. For the cyclic compression tests, the gel sample was compressed to a strain of 20% and then unloaded back to 0. This cycle was repeated for 100 times. Each of the mechanical tests was repeated for three times with distinct samples.

2.4. Swelling capacity

2.4.1. Mass swelling ratio (SR_m)

Classical gravimetric method was used to evaluate the swelling properties of GPG. Briefly, the hydrogel samples were dried to determine their dry weight (W_d). Then immersed dried samples in 37 °C distilled water (simulating physiological environment). And weighted the swollen samples after removing from water (W_s) according to the timepoints. The mass swelling ratio was defined as: $SR_m = [(W_s - W_d)/W_d]$ 100%.

2.4.2. Volume swelling ratio (SR_v)

Freeze-dried certain volume of gel samples (V_d) then immersed into 37 °C distilled water. Freeze-dried and calculated the volume of swollen samples (V_s) according to the timepoints. The volume swelling ratio was defined as: $SR_v = [(V_s - V_d)/V_d]$ 100%.

2.5. Cell culture under mechanical loading

2.5.1. Hydrogel coating

Plates or silicone chambers were coated by a GPG layer with a thickness of 0.5 mm, and sterilized by UV light in hood overnight.
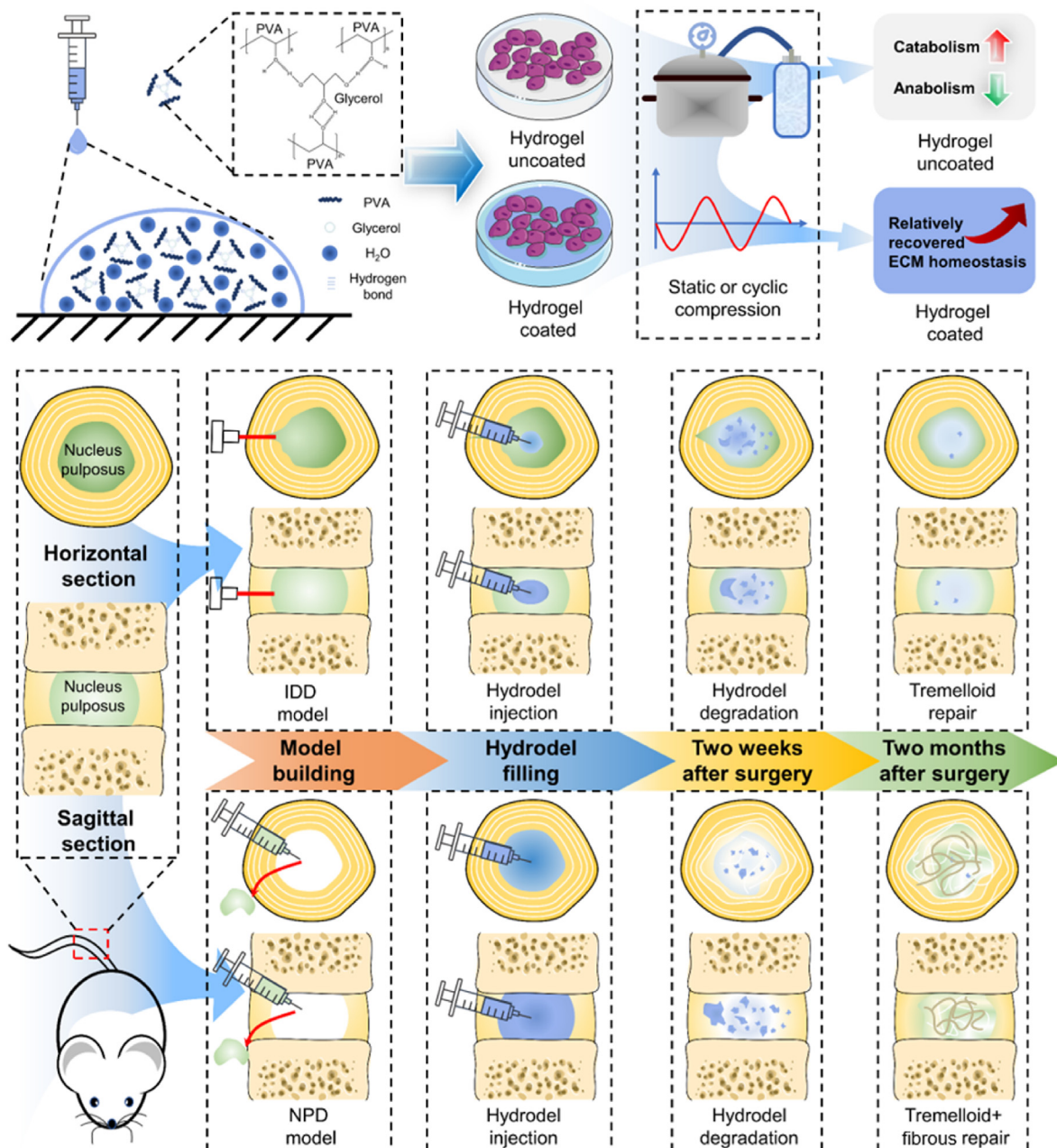
Scheme 1. Schematic illustration of the development of GPG, in vitro cell tests and in vivo animal study.

2.5.2. Hydrostatic loading

The culture system provided hydrostatic stress to NP cells through a compression culture chamber linked with a high-pressure gas cylinder. The samples were subjected to compressive stress at 1 MPa and observed at 0, 24 and 48 h.

2.5.3. Dynamic loading

A loaded cell culture system (Celload-300, Suzhou Haomian Precision Technology Co., Ltd, Suzhou, China) providing adjustable longitudinal cyclic stretching was used to apply mechanical stimuli to NP cells plated on fibronectin/GPG-coated silicone chambers made from poly-dimethylsiloxane (PDMS, Dow Corning, Midland, MI, USA) at an initial density of 3000 cells/cm². NP cells were subjected to cyclic stretching with tensile strain of 20%, 0.2 Hz (pathological strain) or 2%, 2 Hz (pathological frequency) respectively for 6 h. NP cells subjected to static culture without loading were used as the control group (Con).

2.6. NP cells proliferation, viability and apoptosis assay

Rat NP cells (generated and donated by Prof. Di Chen from Shenzhen Institutes of Advanced Technology, Chinese Academy of Sciences) in passage 5–8 were cultured in fibronectin-coated plate with DMEM/F12 (1:1) (DF12; Gibco, Grand Island, NY, United States) containing 10% fetal bovine serum (FBS; Invitrogen, Carlsbad, CA, United States) and 1% antibiotics (penicillin/streptomycin) (Gibco) in a 5% CO_2 incubator at 37 °C. Culture medium was changed every other day. For proliferation assay, NP cells seeded in grouped wells were harvested and cell number was counted at different timepoints (0, 2, 4, 6 days). For viability assay, NP cells seeded on fibronectin/hydrogel-coated plates pre-treated with hydrostatic or dynamic pathological loading were stained by live-dead assay kit (Abcam, ab115347). The live cell dye labeled intact, viable cells green. It was membrane permeant and non-fluorescent until ubiquitous intracellular esterases removed ester groups and rendered the molecule fluorescent. The dead cell dye labeled cells with compromised plasma membranes red. It was membrane-impermeant and bound to DNA with high affinity. Then the percentage of dead cells was quantified. Cell apoptosis was analyzed by detection of DNA fragmentation via a fluorescence assay based on terminal deoxynucleotidyl transferase (TdT)-mediated dUTP nick-end labeling (TUNEL) (one step TUNEL apoptosis assay kit, Beyotime, C1088) and cleaved caspase-3 (Cell Signaling Technology, 9661S) (1:500) immunofluorescence staining. TUNEL and cleaved caspase-3 staining were performed 24 h after 1 MPa of hydrostatic stress treatment on NP cells seeded on plates with or without GPG coating, or 6 h after tensile strain of **20%**, 0.2 Hz or 2%, **2 Hz** cyclic stretching treatment on NP cells seeded on silicone chambers with or without GPG coating respectively. The fluorescence staining results were observed and imaged using fluorescent microscopy (Axio Observer, Zeiss, Germany).

2.7. RNA isolation and quantitative real-time polymerase chain reaction (qRT-PCR)

For qRT-PCR the total RNA kit (Omega Biotek, Norcross, GA, USA) was used to extract RNA and normalized to a cell number. According to the manufacturer's instructions in a 7500 Real-Time PCR System (Applied Biosystems, Foster City, CA, USA) with SYBR Premix Ex Taq (TaKaRa) RT-PCR was performed. The sequences of primers were shown in Table S1. The PCR reaction was conducted using 25 mL of sample cDNA, 2.5 mL deoxyribonucleotide triphosphate (dNTP) mix (2 mM), 2.0 mL MgSO4 (25 mM), 0.5 mL Taq DNA Polymerase (2 U/mL), 2.5 mL 10 PCR buffer, and 15.8 mL deionized H₂O. The reaction mixture was heated to 95 °C for 2.5 min and then amplified for 40 cycles as follows: 95 °C denaturation for 30 s, 50 °C annealing for 30 s, and 65 °C extension for 10 s.

2.8. Western blot assay

Total NP cellular proteins were extracted post mechanical loading treatment using RIPA buffer (Beyotime, Nantong, China) containing protease inhibitors (Beyotime), and quantified using a BCA protein assay kit (Beyotime). Each sample containing 30 mg protein was separated in sodium dodecyl sulfate-polyacrylamide gel (Beyotime) and transferred to nitrocellulose filter membranes (Millipore, Billerica, MA, United States). After blocking for 1 h at 37 °C with 5% skim milk (skim-milk powder in Tris-buffered saline containing 0.1% Tween 20), the membranes were incubated with primary antibodies against Aggrecan (Millipore, AB1031) (1:1000), MMP13 (Abcam, ab39012) (1:1000), and β-actin (Proteintech, 20536-1-AP) (1:2000) at 4 °C overnight. The membranes were washed and incubated with respective horseradish peroxidase-conjugated secondary antibodies at room temperature for 1 h. Finally, the bands were detected with ECL-Plus Reagent (Millipore, Billerica, MA, United States) observed by Amersham Imager 600 (General Electric, United States).

2.9. IDD and NPD surgical procedures

All animal experiments were approved by the Animal Use and Care Committee of the Fourth Military Medical University and conducted in accordance with the National Institute for Health "Guide for the Care and Use of Laboratory Animals", and animal experimentation in this work met the International Guiding Principles for Biomedical Research Involving Animals.

The IDD animal model was established as previously reported [20–22]. Briefly, 30 male Sprague–Dawley rats (8-week-old) in total were used in this study, 15 for IDD and 15 for NPD respectively. The rats in the IDD group were anesthetized with isoflurane and needles (27G) were used to fully puncture the whole layer of annulus fibrosus (AF) through the tail skin, which was confirmed by a trial radiograph. The needle was kept in the disc for about 1 min and length of it was about 5 mm. For Co5/6 (IDD), 5 μl Normal Saline was injected, and for Co6/7 (IDD + Hydrogel), 5 μl hydrogel was injected into disc post puncture. Co7/8 without puncture or injection was set as Con. For NPD models establishment, NP was removed by aspiration after IDD procedure. For Co5/6 (NPD), 20 μl Normal Saline was injected, and for Co6/7 (NPD + Hydrogel), 20 μl hydrogel was injected into disc post NP discectomy. Co7/8 without puncture, NP discectomy or injection was set as Con. 1/3 rats of IDD and NPD groups were harvested at 2 weeks, 2 months and 6 months post-surgery respectively.

2.10. Histology

4% paraformaldehyde was used to fix the spine samples of rats for 48 h, then washed and decalcified in 15% ethylenediaminetetraacetic acid (EDTA; pH = 7.4) for about 4 weeks. Embedded decalcified samples with paraffin. Midsagittal-oriented sections (7 μm) were prepared for histological staining. Safranin O (SO) staining were performed by using staining kit according to standard protocols (Solarbio, Beijing, China). Histological scores were assessed as described previously [23]. Briefly, the entire slides for each IVD were stained with Safranin O and scored by two observers who were blinded to the animal treatments. The scale is based on 5 categories of degenerative changes (1. Cellularity of the anulus fibrosus; 2 Morphology of the anulus fibrosus; 3. Border between the anulus fibrosus and nucleus pulposus; 4. Cellularity of the nucleus pulposus; 5. Morphology of the nucleus pulposus) with scores ranging from 5 points (1 in each category) for a normal disc to 15 points (3 in each category) for a severely degenerated disc. For immunofluorescence staining, sections were incubated with Aggrecan (Millipore, AB1031) (1:100) at 4 °C overnight, followed by secondary antibodies (1:200) at 37 °C for 2 h and finally incubated with DAPI (Beyotime, C1002) for 2 min. Each step was followed by washing with PBS three times for 5 min. The sections were observed under a fluorescence microscope (Axio Observer, Zeiss, Germany).

2.11. Statistical analysis

The results were given as means ± SD. Statistical analyses were performed using SPSS 22.0 and GraphPad Prism 7.0 software. Differences between two groups were analyzed by Student's t-test, while differences among multiple groups were analyzed by one-way analysis of variance followed by Tukey's multiple-comparison post hoc test. Statistical significance was set at $p < 0.01$.

3. Results

3.1. Preparation and characterization of GPG

As shown in Fig. 1a, it is proposed that glycerol molecules formed multiple H-bonds with PVA, thereby functioned as bridge molecules to connect PVA chains into 3D networks, eventually leading to the formation of a hydrogel. The relatively weakness of the glycerol-mediated crosslinking provided an effective energy-dissipating mechanism, leading to the excellent energy absorbing capability of the hydrogel.

Fourier transform infrared spectroscopy (FTIR) analysis was performed to reveal the interaction of PVA chains with glycerol in GPG network. The FTIR spectra of pure PVA and GPG were shown in Fig. 1b. For pure PVA, the broad and strong absorption peak at 3420 cm^{-1} ascribed for the –OH stretching vibration, and the absorption peak at 1116 cm^{-1} corresponded to the C–O stretching vibration. Compared with pure PVA, the –OH stretching peak, C–O stretching vibration peak of the hydrogel shifted from 3420 cm^{-1} and 1116 cm^{-1} to 3385 cm^{-1} and 1101 cm^{-1} respectively. This indicated the formation of H-bond between glycerol molecules and PVA chains, which was stronger than those in the pure PVA.

GPG could be injected from needle (27G) (Fig. 1c), indicating a high injectability that enables the treatment of IVDD through a minimally invasive approach. The wettability of GPG was examined by the contact angle measurement [24]. As shown in Fig. 1d, the water contact angle on the surface of GPG (26.46 ± 0.26°) was significantly lower than pure PVA (55.48 ± 0.34°), indicated a higher hydrophilicity of GPG than PVA.

### 3.2. GPG had NP-like viscoelastic characteristics and good mechanical properties

Rheological test was performed on GPG to evaluate its viscoelastic characteristic. As shown in Fig. 2a, in the frequency range of 0.1–10 Hz, the storage modulus (G') of the GPG kept constant while the loss modulus (G") decreased slightly with increasing frequency, and hence the loss factor (G"/G') gradually decreased. In the whole frequency range, the G' was much larger than the corresponding G", and G"/G' was less than 0.1, suggesting an elastic characteristic of the gel. Importantly, the G' and G" of the GPG were both comparable to those of native NP [25], indicating the rheological property of GPG well matched with that of NP.

The static compression test was performed to evaluate the compressive property of GPG (Sup. Fig. 1). The results demonstrated that the GPG could be compressed to a strain of 69.1 ± 2.2% until failure, indicating a high ductility. And the compressive modulus of GPG is 4.4 ± 0.2 kPa, matching well with that of the healthy NP [26]. Cyclic compression test at 20% maximum compressive strain were conducted to evaluate the mechanical property of GPG under dynamic compressive loading. As shown in Fig. 2b, after the first cycle, the subsequent nine stress–strain curves almost remained overlapped and showed minimal energy dissipation. And little deformation was observed after the cyclic compressive test (Fig. 2c). A significant energy dissipation of the gel was observed during the continuous cyclic compression for up to 100 cycles, suggesting an energy absorbing capability. Importantly, we found that the hydrogel could fully recover from a large deformation within 5 min post-press (Fig. 2d), which demonstrated the self–recovery properties of GPG after deformation.

Overall, the above results demonstrated that GPG had a NP-mimetic
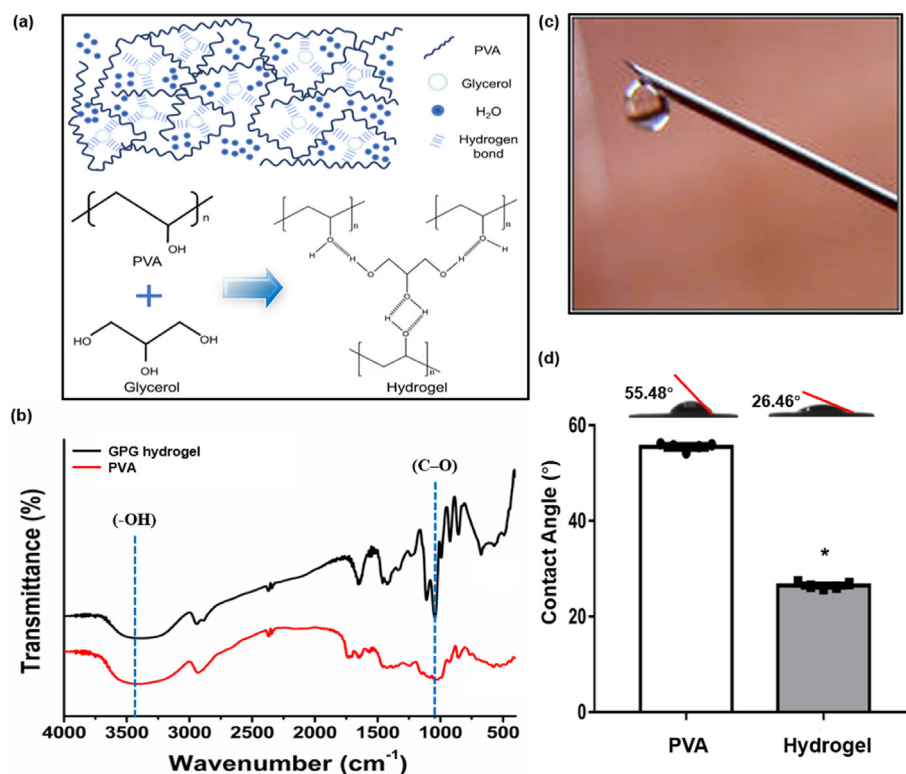
Fig. 1. Preparation and characterization of GPG. (a) Schematic diagram showing the structure and the cross-linking mechanism of GPG. (b) FTIR spectra of PVA and GPG. (c) Photo showing the injectability of GPG through a 27 G syringe needle. (d) Quantification of contact angle measurement. The lower contact angle indicates a higher hydrophilicity.
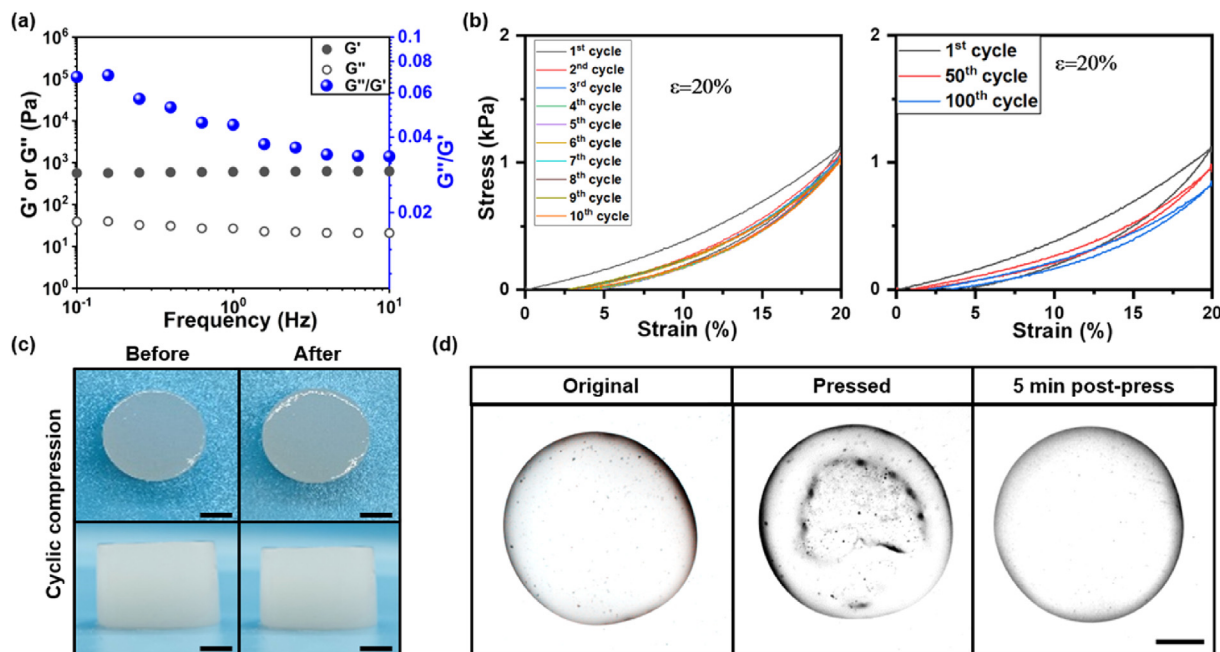
Fig. 2. Rheological and mechanical properties of GPG. (a) Dependence of G', G'' and the G''/G' ratio of GPG on the frequency of oscillation in rheological test. (b) Stress–strain curves of the GPG at different compression cycles up to 100 cycles. Tests were performed at a maximum strain of 20% under the displacement rate of 10 mm min^{-1}. (c) Photos of GPG sample before and after cyclic compression test. Scale = 5 mm. (d) Hydrogel sample recovered within 5 min post press. Scale = 2 mm.
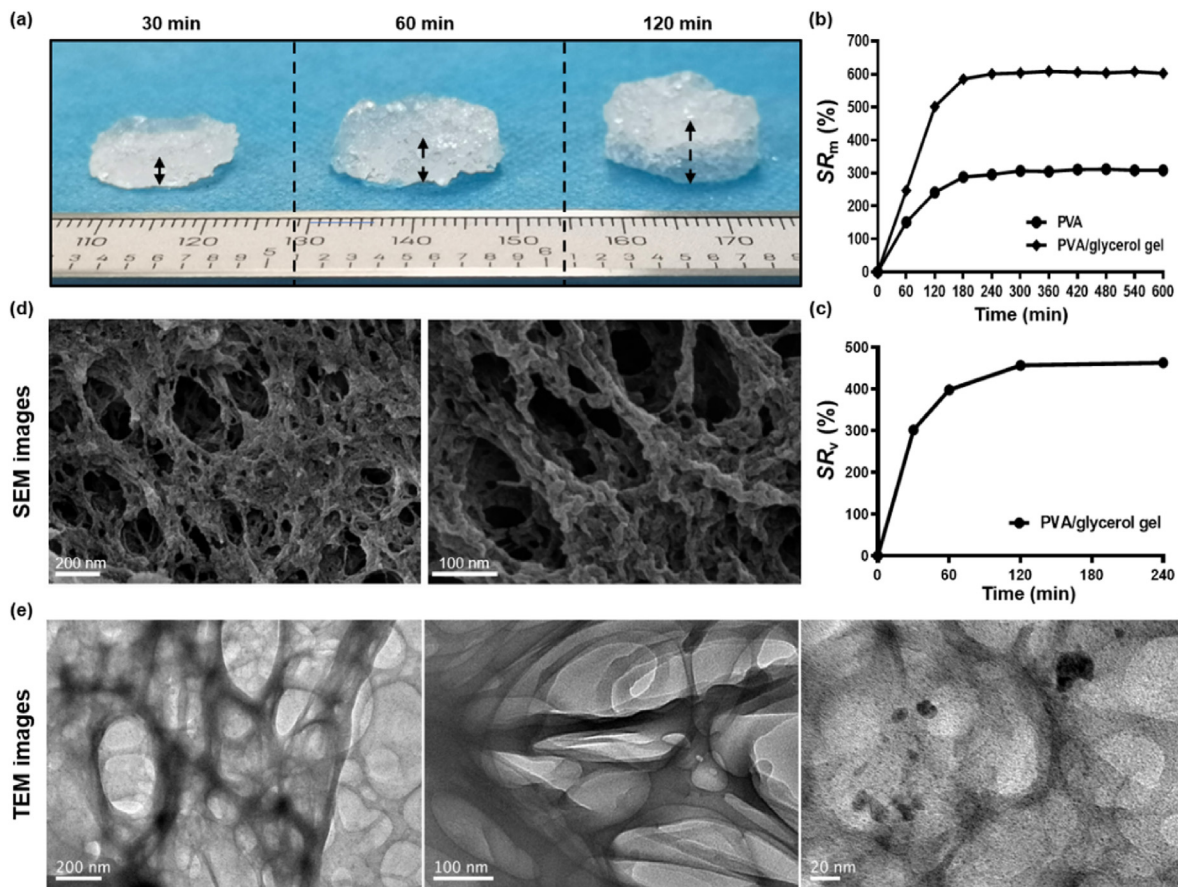
Fig. 3. Swelling capacity and network structure of GPG. (a) Photos of freeze-dried GPG samples after being placed into distilled water for various time periods. (b) Mass swelling ratio curves of pure PVA and GPG. (c) Volume swelling ratio curves of GPG. (d) SEM and (e) TEM images of freeze-dried GPG.

viscoelastic property, energy dissipation and self-recovery capability.

3.3. GPG had high swelling capacity and highly porous structure

The swelling behaviors of GPG were shown in Fig. 3. Visually, all the gel samples swelled time-dependently after being placed into the distilled water (Fig. 3a). To determine the swelling capacity of GPG, mass swelling ratio (SR_m) and volume swelling ratio (SR_v) were calculated. The swollen weight (W_s) was measured per hour until 10 h after immersing. The corresponding SR_m was calculated and presented in Fig. 3b. To analyze the swelling trends, lines were drawn between the measurement values, from which it could be seen the SR_m increased dramatically, on other word, all the samples absorbed water rapidly in the initial swelling stage. The water absorption of GPG was faster than PVA hydrogel, which could be explained that more porous structures made water molecules transfer easier between the GPG matrix and the external aqueous phase. GPG and PVA hydrogel swelled up to maximum and reached dynamic equilibrium at about 3 h after immersing. The maximum SR_m of GPG (608.67 ± 0.52%) was 1.9 times higher than PVA hydrogel (295.67 ± 0.18%) (Fig. 3b). The swelling could also be described by the volume swelling ratio (SR_v). The SR_v curve of GPG showed the similar trend with its SR_m, indicating that swelling induced deformation significantly increased at the early swelling stage and reached its maximum volume expansion at about 2 h after placed into water (Fig. 3c).

The swelling ability of hydrogel could not be simply related to the hydrophilia of components, since the morphology of the crosslinking network also played an essential role in regulating the capacity of water sorption [27]. To clarify the micro-architecture of GPG, Scanning Electron Microscope (SEM) and Transmission Electron Microscope (TEM) were used to observe the superficial and inside structures. Images were taken at random locations across the hydrogel samples. The SEM and TEM images both demonstrated that the hydrogel had a porous-network structure with circular pores which varied greatly in diameter (Fig. 3d

and e). This kind of gel morphology contributed to the hydrophilic nature, swelling degree, cell migration, deformation resistant and recovery properties which were critical factors for an IVD biomimetic material [28].

3.4. GPG preserved NP cells vitality against pathological loading

Biocompatibility was tested through culturing NP cells with GPG serving as plate coating, and monitoring the vitality of cells. The results showed that GPG coating did not affect NP cells morphology, proliferation or vitality, suggesting a high biocompatibility (Sup. Fig. 2).

To investigate the functions of hydrogel on NP cells under pathological loading, NP cells cultured on hydrogel coating or plate (control group) were subjected to hydrostatic stress at 1 MPa. We observed that 1 MPa of hydrostatic loading dramatically stimulated NP cells death and reduced their proliferation in control group, while hydrogel coating significantly ameliorated these pathological changes (Fig. 4a, b, c). Excessive loading also up-regulated the expression level of catabolic markers (*MMP-13*, *ADAMTS-5*), and down-regulated the expression of anabolic markers (*Aggrecan*, *Collagen II*) of NP cells, while hydrogel coating efficiently reversed these degenerated phenomena by maintaining the level of anabolic genes and down-regulating the level of catabolic genes (Fig. 4d). The therapeutic effects were further confirmed at protein level that hydrogel coating obviously reduced the amount of MMP-13 and maintained the amount of Aggrecan and Collagen II (Fig. 4e). These results indicated that GPG could protect NP cells vitality under pathological hydrostatic-loading environment.

To investigate the protective ability of hydrogel under harmfully dynamic loading environment, NP cells were cultured on elastic substrates with or without hydrogel coating, which were applied with cyclic stretching at abnormal frequency (**2 Hz**, 2%) or strain (0.2 Hz, **20%**). The results revealed that aberrant loading frequency or strain reduced proliferation and stimulated cell death independently, while hydrogel
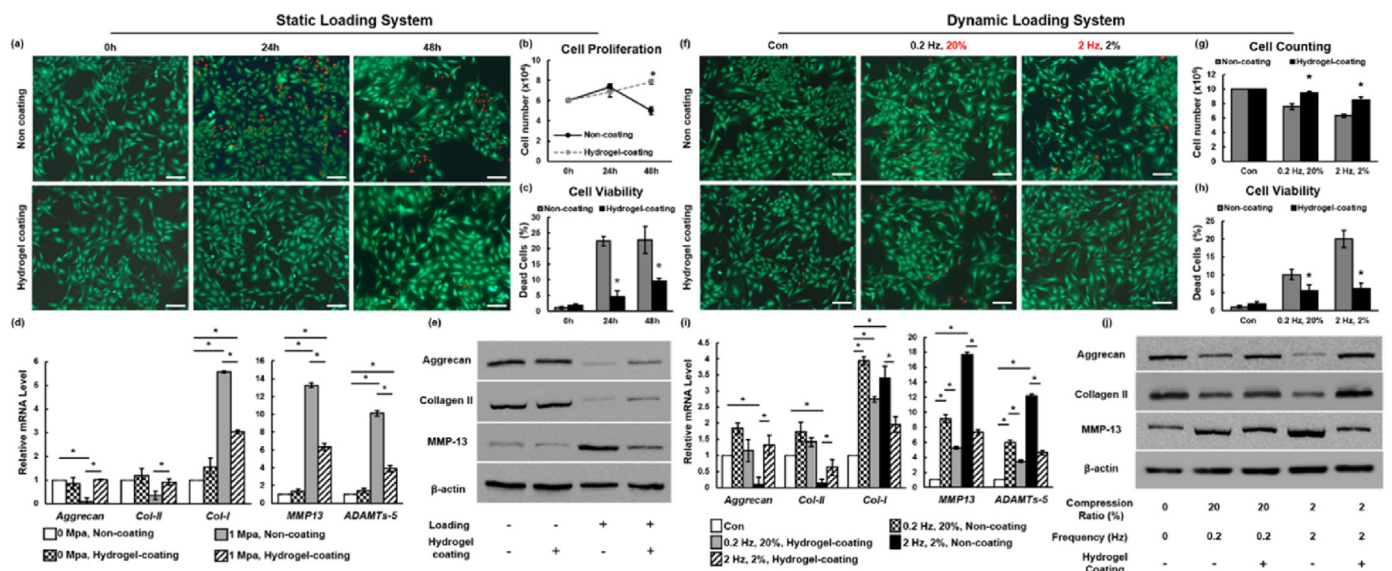
Fig. 4. GPG protected NP vitality against pathologically hydrostatic and dynamic stresses. (a) NP cells were seeded on plates with or without GPG coating, then subjected to 1 MPa of hydrostatic stress. Live-dead staining was performed on the indicated timepoints. Red: Dead cells. (b) Proliferation curves were drawn according to cell counting on the indicated timepoints. (c) Cell viability assay: Quantification of the percentage of dead cells. (d) qRT-PCR results of *Aggrecan, Col-II, Col-I, MMP-13* and *ADAMTs-5* relative mRNA level of NP cells treated with 1 MPa of hydrostatic stress for 24 h. (e) Aggrecan, Collagen II and MMP-13 protein content of the NP cells treated with 1 MPa of hydrostatic stress for 24 h were detected by western blot. NP cells cultured in plates without GPG coating or loading stimulation were set as control. (f) NP cells were seeded on silicone chambers with or without GPG coating, then subjected to cyclic stretching with tensile strain of 20%, 0.2 Hz or 2%, 2 Hz respectively for 6 h. Live-dead staining was performed after the dynamic compression treatment. Red: Dead cells. (g) Cell counting was performed after dynamic compression treatment. (h) Cell viability assay: Quantification of the percentage of dead cells. (i) qRT-PCR results of *Aggrecan, Col-II, Col-I, MMP-13* and *ADAMTs-5* relative mRNA level of NP cells after dynamic compression treatment (j) Aggrecan, Collagen II and MMP-13 protein content of NP cells after dynamic compression treatment were detected by western blot. NP cells cultured in silicone chambers without GPG coating or loading stimulation were set as control. n = 3 per group per timepoint. Scale = 50 μm *: p < 0.01.

coating significantly ameliorated these pathological changes (Fig. 4f, g, h). Moreover, aberrant loading frequency or strain up-regulated the expression of catabolic genes (*MMP-13, ADAMTS-5*), and down-regulated the expression of anabolic genes (*Aggrecan, Collagen II*) of NP cells, which could be attenuated by hydrogel coating (Fig. 4i). Western blot analysis further demonstrated the protective effects of GPG on NP cells metabolism at protein level (Fig. 4j).

To further analyze the effects of GPG on NP cell apoptosis, we performed TUNEL and cleaved caspase-3 staining. The results revealed that both pathologically hydrostatic pressure and abnormal dynamic stress stimulated NP cell apoptosis, while GPG coating obviously attenuated these changes (Sup. Fig. 3).

3.5. GPG maintained IVD height and CEP structure in IDD and NPD models

To evaluate the therapeutic effects of GPG injection on IVD lesion in vivo, needle puncture (IDD) and NP discectomy (NPD) models were adopted. IDD as a classic model mimicking IVDD process was set up

through needle puncture of AF. And NPD model was established by NP discectomy to simulate NP defect post-surgery. μCT scanning was performed 2 months after surgery. For IDD models, AF damage caused by needle puncture induced significant IVD height decrease (68.7% of Con), which was almost completely inhibited by GPG injection (97.2% of Con). CEP destruction was found in 20% IVD samples while none in GPG injection group (Fig. 5a, b, c). For NPD models, NP discectomy indued dramatic IVD collapse (19.9% of Con) with severe CEP destruction in 60% IVD samples. GPG injection greatly maintained IVD height (94.8% of Con) and physiological CEP structure (Fig. 5d, e, f).

3.6. GPG ameliorated water content lost in IDD and NPD models

MRI was also performed 2 months after surgery to assess the structure and water content of IVDs in various groups. For IDD models without treatment, punctured IVDs showed significant NP damage (4.75 times higher than Con by Pfirrmann Grading) and decrease in the MRI index (36.1% of Con), indicating the loss of water content in IVD degeneration progress. Hydrogel injection well maintained NP morphology (2.5 times
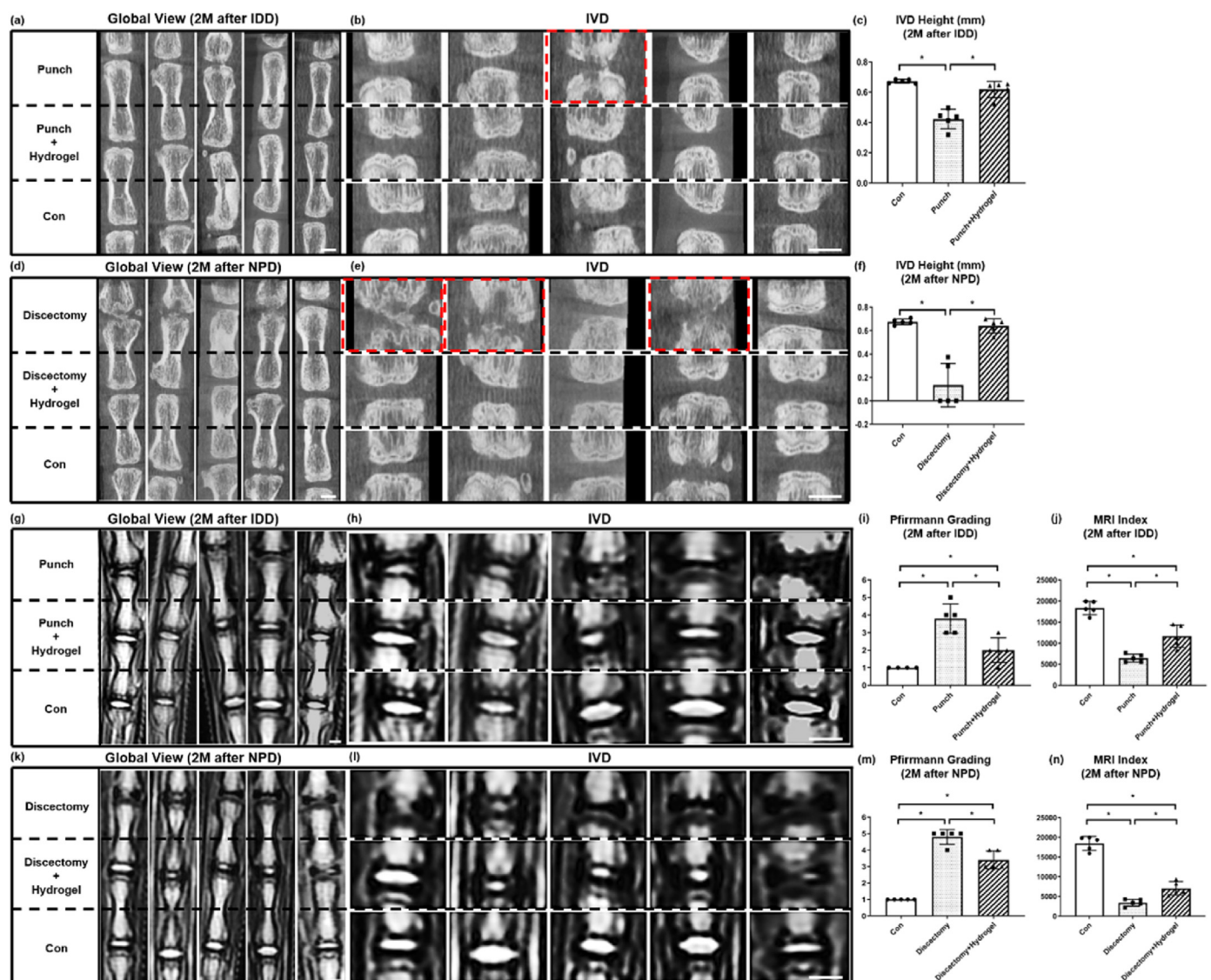
Fig. 5. GPG preserved IVD height, CEP structure and water content in IDD and NPD models at 2 months after surgery. (a) Micro-CT images (Global view) of different groups in IDD models. (b) Magnified images of (a). (c) Quantification of IVD height of IDD models. (d) Micro-CT images (Global view) of different groups in NPD models. (e) Magnified images of (d). (f) Quantification of IVD height of NPD models. Red label: Destructed CEP. (g) MRI images (Global view) of different groups in IDD models. (h) Magnified images of (g). (i) Pfirrmann Grading of IDD models (j) MRI index of IDD models (k) MRI images (Global view) of different groups in NPD models (l) Magnified images of (k) (m) Pfirrmann Grading of NPD models (n) MRI index of NPD models. n = 5 per group per timepoint. Scale = 2 mm *: p < 0.01.

higher than Con by Pfirrmann Grading) and water content (MRI index: 69.4% of Con) (Fig. 5g, h, i, j) compared to non-treated IDD. For NPD models, NP discectomy induced dramatic IVD destruction (4.8 times higher than Con by Pfirrmann Grading), and a total loss of water contend (19.4% of Con). while hydrogel injection slightly but significantly ameliorated water loss (MRI index: 41.7% of Con) and destruction (3.4 times higher than Con by Pfirrmann Grading), particularly maintaining the morphology of CEP (Fig. 5k, l, m, n), compared to non-treated NPD.

3.7. GPG assisted tremelloid repair in IDD models

Safranin' O staining was performed to evaluate histological changes of NP. Two weeks after surgery, as shown in Fig. 6a, the number of NP cells significant decreased and less ECM was preserved in non-treated IDD group. The histological score of the IDD group was 3.14 times higher than Con, suggesting a severe degeneration. Treatment by GPG injection significantly alleviated IDD phenotype with a relatively lower histological score (2.14 times higher than Con) (Fig. 6b) that non-treated IDD group. Injected hydrogel partially degraded and absorbed could be observed from puncture site to the whole area mixed with NP tissue. Two months after surgery, as shown in Fig. 6c, severe NP damage accompanied with AF destruction could be observed in puncture group. While GPG injection, which was almost degraded and absorbed, greatly maintained the IVD morphology (Fig. 6d).

3.8. GPG maintained NP homeostasis by promoting the anabolism of ECM

2 weeks after surgery, histological results revealed that injected hydrogel mixed with NP tissue was partially degraded and absorbed, while hydrogel efficiently maintained IVD height, the number of NP cells and the amount of ECM compared with IDD group (Sup. Fig. 4a, e). IF staining showed aggrecan dramatically lost in IDD group (Sup. Fig. 4b, c, d). However, in hydrogel injection group, aggrecan accumulated surrounding or overlapping with remaining hydrogel, indicating that GPG maintained NP homeostasis by promoting the anabolism of ECM (Sup. Fig. 4f, g, h).

3.9. GPG stimulated fibrous repair in NPD models

As shown in Fig. 6, IVD collapsed 2 weeks after surgery and totally destructed accompanied by AF damage, inflammatory hyperplasia and CEP invaded 2 months after surgery without the support of NP (Fig. 6e, f, g). Hydrogel injection did not reverse IVD morphological changes but effectively supported IVD height and CEP structure by stimulating fibrous repair in NP area which induced a slightly but significantly lower

histological score of hydrogel injection group compared with NPD group (Fig. 6h).

3.10. GPG showed a long-term therapeutic effect in IDD and NPD models

To evaluated the long-term therapeutic effect of GPG injection, MRI was performed 6 months after treatment of IDD and NPD. Hydrogel injection significantly ameliorated AF puncture induced morphological changes, height reduction and water loss of IVD (Fig. 7a–e). MRI results of NPD group showed that NP discectomy induced extremely severe destruction of IVDs, including a total loss of water content, IVD collapse, destroyed CEP, and even vertebral fusion. Notably, hydrogel injection effectively protected CEP integrity, partially preserved IVD height and water content compared with non-treated NPD group (Fig. 7f–j). As shown in Supplementary Fig. 5, histological staining was performed for morphological observation. For IDD models, AF damage induced obvious NP fibrosis, CEP vanishment and IVD collapse. For NPD models, much more severe destructions were observed, including inflammatory hyperplasia, invaded growth plate at both sides and even IVD fusion. While GPG injection partially maintained IVD morphology and structure by stimulating tremelloid repair in IDD and fibrous repair in NPD models.

4. Discussion

The current surgical approaches for the alleviation of severe LBP, such as spinal fusion and discectomy, can barely restore the spinal biomechanics to healthy condition, and may even induce further IVDD at the initially affected spinal segment or adjacent IVDs, due to their anatomical position hardly accessible for surgical repair without mechanical damage to their surrounding tissues and original structure [29]. As a result, the demand of minimally invasive strategies to treat spinal diseases without fusion or discectomy has rapidly increased in recent years [30]. The ultimate goal of an ideal approach for treating LBP is to restore the motion and mechanical state to normal physiological conditions besides pain relief. NP replacement with injectable synthetic materials targeting earlier stages of IVDD may help to preserve the AF and be more amenable to minimally invasive surgical techniques.

Injectable hydrogels bear great potential in the treatment of IVDD due to its special characteristics including the adaptability to defect shape or size, quick gelation and construction for uniform distribution and high moisture content to mimic native NP [31]. However, NP property, varying with the degeneration and mechanical states, is described with a wide range from fluid to isotropic solid [32]. Most reported hydrogels for treatment of IVDD are not able to mimic the mechanical properties of native NP and are difficult to provide sustainable mechanical support in
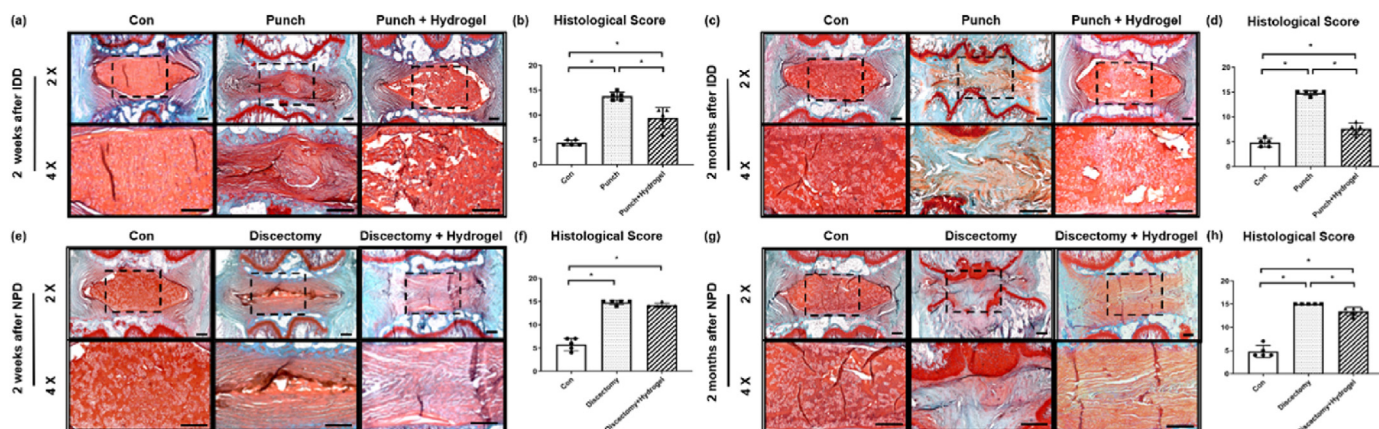
Fig. 6. GPG stimulated tremelloid repair in IDD and fibrous repair in NPD models. (a) Safranin' O staining of IVD at 2 weeks after IDD surgery. (b) Histological score of (a). (c) Safranin' O staining of IVD at 2 months after IDD surgery. (d) Histological score of (c). (e) Safranin' O staining of IVD at 2 weeks after NPD surgery. (f) Histological Score of (e). (g) Safranin' O staining of IVD at 2 months after NPD surgery. (h) Histological Score of (g). n = 5 per group per timepoint. Scale = 200 μm *: p < 0.01.
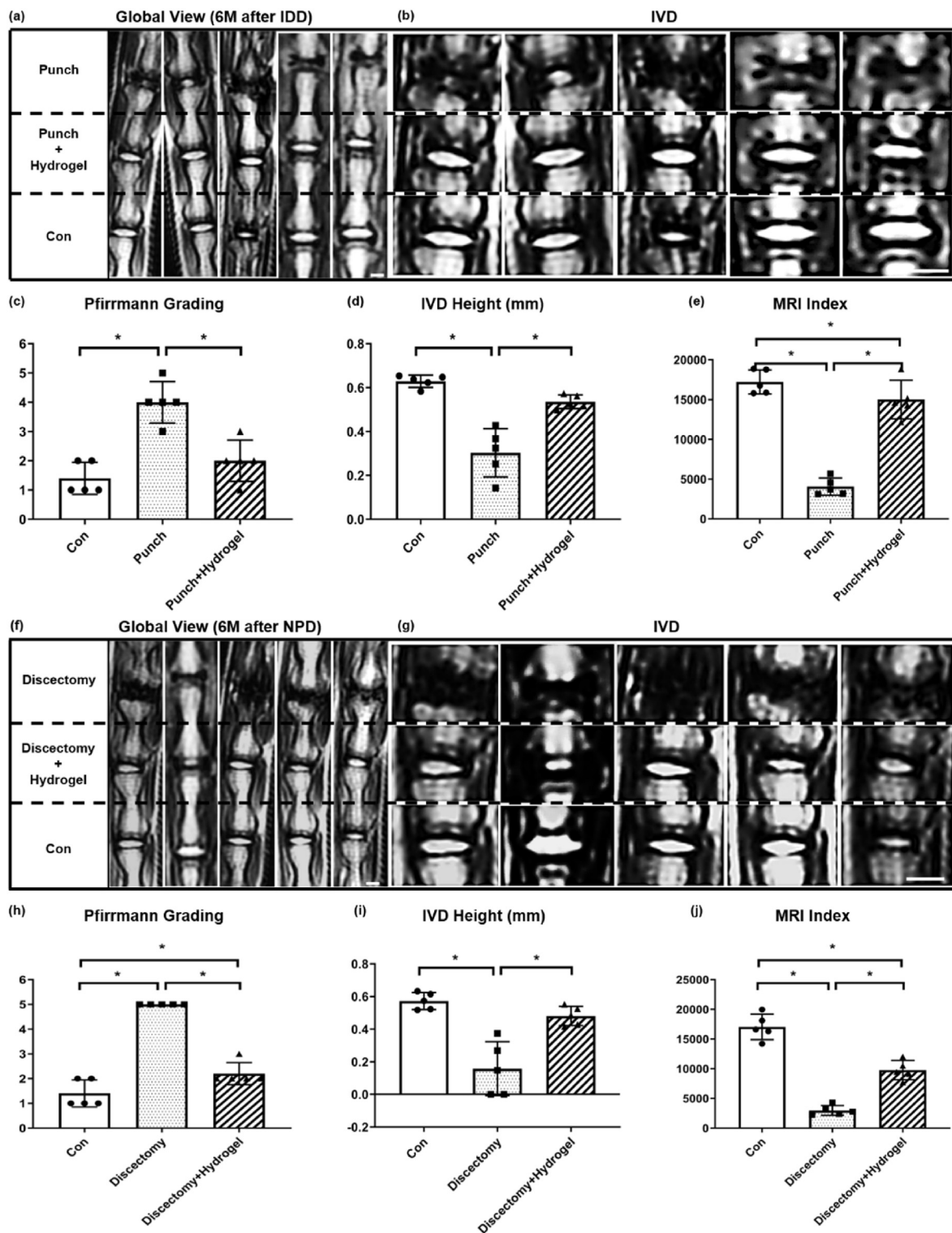
Fig. 7. GPG showed an ideal long-term therapeutic effect in IDD and NPD models at 6 months after surgery. (a) MRI images (Global view) of different groups in IDD models. (b) Magnified images of (a). (c) Pfirrmann Grading of IDD models. (d) Quantification of IVD height of IDD models. (e) MRI index of IDD models. (f) MRI images (Global view) of different groups in NPD models. (g) Magnified images of (f). (h) Pfirrmann Grading of NPD models. (i) Quantification of IVD height of NPD models (j) MRI index of NPD models. n = 5 per group. Scale = 2 mm *: p < 0.01.

the complicated mechanical environment of IVD. To resolve these issues, our study aimed to synthesize an injectable hydrogel that mechanically mimics the native NP tissue for absorbing and transferring load to support the structural integrity of IVD.

A physically crosslinked gel was developed with PVA and glycerol via a facile one-pot method, ensuing a high translational potential. The as-

prepared GPG exhibited a high injectability which was enabled by the shear-thinning behavior due to reversible H-bonds. Compared with in-situ gelation hydrogels, the GPG-based strategy has better reliability and bio-safety during injection. The rheological test results suggested a solid gel characteristic of the GPG, and the G' and G" of the gel were both comparable to those of native NP. Moreover, the gel was able to

withstand the cyclic compressive loading and exhibits an effective energy-dissipating capability, which should be due to the dynamic damage/recovery of the reversible H-bonds between PVA chains and glycerol. Minimal geometrical change of the hydrogel was observed after continuous compression cycles. The unique mechanical properties of GPG ensured its durable strengthening and energy-absorbing function to support the IVD height and structural integrity confronting constant compressive loading induced by motion and weight bearing. Swelling capacity, which is defined by swelling rate (mass/volume) and affected by the internal porosity, primarily characterizes the hydrophilicity and the internal cross-linking density [28,33]. A highly porous structure with interconnected pores of GPG was revealed by the SEM and TEM images. This microstructure indicated an ideal swelling capacity of the gel, which was confirmed by swelling ratio analysis, moreover provided potential of facilitating cell spreading and migration, deformation resistant, signal transformation process, controlled release and recovery properties [34]. For tissue engineering materials, it is a general requirement that cells adhere to the surface of scaffolds and maintain the capability of proliferation [35]. The in vitro culture results suggested that GPG did not inhibit NP cells proliferation or vitality, indicating a high biocompatibility.

NP cells have been found vulnerable to compression, flexion, axial rotation of spine and complex loading mechanisms through both one impact, and continuously cyclical loading [36]. To simulate chronic loading, which has been reported to be able to induce IVDD, we cultured NP cells within 1 MPa hydrostatic pressure [37]. A dramatic increase of apoptotic and floating dead cells was found after 24 h pressure treatment, which was not observed in hydrogel coated dishes, indicating that the hydrogel preserved NP cells vitality by reducing apoptosis and enhancing cellular attachment [38]. Pathologically dynamic loading out of the physiological range of frequency (0.2–1.2 Hz) or compressive deformation (<15%) also stimulates IVDD [39,40]. The GPG coating effectively protected NP cells vitality in both pathologically dynamic loading environments with abnormal frequency and compressive deformation. In NP, mechanical stimuli system originating from the cell environment, through neighbouring cells, ECM, fluid flow, cell interior cytoskeletal rearrangements, or osmotic forces, maintains NP cells metabolism [17]. While the balance of this system is destructed in IVDD [34]. In our study, the hydrogel functioned as normal ECM to provide NP cells beneficial environment to dissipate abnormal energy, enhance cellular attachment, maintain highly hydrated and facilitate cellular substance exchange, as a result, preserved the expression of anabolic markers and downregulated catabolic markers stimulated by pathological loading. The upregulated expression of *Col I* in excessive loading, frequency and deformation groups indicated that pathologically mechanical stimuli might induce fibroblastic differentiation, while hydrogel coating partially maintained the homeostasis and characteristics of NP cells.

After observing these promising results in vitro, two animal models (IDD and NPD) were adopted to evaluate the therapeutic effects of GPG injection on IVD lesion in vivo [41]. As detected by MRI and μCT, GPG injection effectively preserved water content in IDD discs, and partially rescued the total loss of water in NPD discs, moreover, restored IVD height in both models. The degeneration or sclerosis of the CEP, which can resist intervertebral pressure and allow nutrient diffusion, may induce metabolic disorder in the disc [42]. We observed pathological CEP changes in both models 2 months after surgery, especially in NPD group, in which all the IVDs after discectomy had severe destruction. While, GPG injection protected CEP morphological and structural integrity. Histological results of IDD models 2 weeks after surgery showed early-stage IVDD morphologies involving loss of proteoglycans and disorganization of the collagen fiber network within the AF [43]. The hydrogel, partially degraded and absorbed, efficiently preserved the number of NP cells and the amount of aggrecan, indicating its function of maintaining NP homeostasis by promoting the anabolism of ECM. Interestingly, the hydrogel injection stimulated fibrous repair in NPD discs. Previous studies revealed a possible migratory pathway for NP

repairment or regeneration, biologically dynamic loading played an inductive role by attracting endogenous cells from the stem cell niches and directing them to commit to fibroblastic differentiation [44]. Therefore, we suspected that NP discectomy induced IVD immobilization or even fusion, while the hydrogel rebuilt the dynamic mechanical environment contributing to the equilibrium of water and nutrition exchange, and the migration and regeneration of endogenous cells [45]. Not sufficiently but significantly, we further proved a long-term therapeutic effect of GPG injection by analyzing both models 6 months after surgery. Nevertheless, a longer time of follow-up study is still necessary. According to our studies, GPG injection should be considered as a novel direction for treating IVDD induced by AF damage or NP defect.

5. Conclusions

An injectable hydrogel (GPG) was prepared by glycerol-mediated crosslinking of PVA chains. GPG had a porous structure and fast swelling capacity. The storage modulus and compressive modulus of the hydrogel were both comparable to those of native NP. Meanwhile, GPG was able to withstand cyclic loading and exhibited an effective energy dissipation ability. In vitro studies indicated that GPG had protective functions on the NP cell vitality against pathologically mechanical loading. And in vivo studies demonstrated a long-term therapeutic effect of GPG on IVD repair both in IDD and NPD models. It is concluded that the low cost, cell- and drug-free, injectable GPG bears great translational potential for the clinical treatment of IVDD via a minimally invasive approach.

Ethic statement

The animal study was reviewed and approved by Animal Use and Care Committee of the Fourth Military Medical University. Ethical approval was obtained from the Institutional Review Board of Xijing Hospital of the Fourth Military Medical University (KY20203146-1).

Authors' contribution

HJ, XL, LiY, ZL and LY designed the experiments. HJ, XL, DoW, JW, QS, XH, KW, BZ, PP, HW, DW carried out most of the experiments. QS, XH, PP, HW, DW and PL helped collecting the samples. HJ, XL, DoW, JW, QS, XH, BZ, KW, PL analyzed data. XL, DoW proofread the manuscript. HJ, XL, LiY, ZL and LY supervised the experiments and wrote the paper. All authors contributed to the article and approved the submitted version.

Declaration of competing interest

The authors declare that the research was conducted in the absence of any commercial or financial relationships that could be construed as a potential conflict of interest.

Acknowledgments

Appendix A. Supplementary data

Supplementary data to this article can be found online at https://doi.org/10.1016/j.jot.2022.03.006.

References

[1] Knezevic NN, Candido KD, Vlaeyen JWS, Van Zundert J, Cohen SP. Low back pain. Lancet 2021;398(10294):78–92.

[2] Hartvigsen J, Hancock MJ, Kongsted A, Louw Q, Ferreira ML, Genevay S, et al. What low back pain is and why we need to pay attention. Lancet 2018;391(10137): 2356–67.

[3] Vergroesen PP, Kingma I, Emanuel KS, Hoogendoorn RJ, Welting TJ, van Royen BJ, et al. Mechanics and biology in intervertebral disc degeneration: a vicious circle. Osteoarthritis Cartilage 2015;23(7):1057–70.

[4] Owen PJ, Hangai M, Kaneoka K, Rantalainen T, Belavy DL. Mechanical loading influences the lumbar intervertebral disc. A cross-sectional study in 308 athletes and 71 controls. J Orthop Res 2021;39(5):989–97.

[5] Desmoulin GT, Pradhan V, Milner TE. Mechanical aspects of intervertebral disc injury and implications on biomechanics. Spine 2020;45(8):E457–64.

[6] Newell N, Little JP, Christou A, Adams MA, Adam CJ, Masouros SD. Biomechanics of the human intervertebral disc: a review of testing techniques and results. J Mech Behav Biomed Mater 2017;69:420–34.

[7] Foster NE, Anema JR, Cherkin D, Chou R, Cohen SP, Gross DP, et al. Prevention and treatment of low back pain: evidence, challenges, and promising directions. Lancet 2018;391(10137):2368–83.

[8] Peng B. Issues concerning the biological repair of intervertebral disc degeneration. Nat Clin Pract Rheumatol 2008;4(5):226–7.

[9] Skalli W, Dubousset J. Intervertebral disc transplantation. Lancet 2007;369(9566): 968–9.

[10] Chen Y, Yang H, Wang Y, Zou J. Relationship of endplate changes and low back pain after discectomy. Clin Neurol Neurosurg 2019;184:105449.

[11] Ruan D, He Q, Ding Y, Hou L, Li J, Luk KD. Intervertebral disc transplantation in the treatment of degenerative spine disease: a preliminary study. Lancet 2007; 369(9566):993–9.

[12] Ai C, Lee YHD, Tan XH, Tan SHS, Hui JHP, Goh JC. Osteochondral tissue engineering: Perspectives for clinical application and preclinical development. J Orthop Translat. 2021;30:93–102. https://doi.org/10.1016/j.jot.2021.07.008.

[13] Leone G, Consumi M, Lamponi S, Bonechi C, Tamasi G, Donati A, et al. Thixotropic PVA hydrogel enclosing a hydrophilic PVP core as nucleus pulposus substitute. Mater Sci Eng C Mater Biol Appl 2019;98:696–704.

[14] Bowles RD, Setton LA. Biomaterials for intervertebral disc regeneration and repair. Biomaterials 2017;129:54–67.

[15] Tang TT, Qin L. Translational study of orthopaedic biomaterials and devices. J Orthop Translat 2016;5:69–71.

[16] Qi C, Yan X, Huang C, Melerzanov A, Du Y. Biomaterials as carrier, barrier and reactor for cell-based regenerative medicine. Protein Cell 2015;6(9):638–53.

[17] Joshi A, Fussell G, Thomas J, Hsuan A, Lowman A, Karduna A, et al. Functional compressive mechanics of a PVA/PVP nucleus pulposus replacement. Biomaterials 2006;27(2):176–84.

[18] Shuijiao Peng, Shuxuan Liu, Yujun Sun, Nanping Xiang, Xiancai Jiang, Linxi Hou. Facile preparation and characterization of poly(vinyl alcohol)-NaCl-glycerol supramolecular hydrogel electrolyte. Eur Polym J 2018;106:206–13. https://doi.org/10.1016/j.eurpolymj.2018.07.024.

[19] Bader RA, Rochefort WE. Rheological characterization of photopolymerized poly(vinyl alcohol) hydrogels for potential use in nucleus pulposus replacement. J Biomed Mater Res 2008;86(2):494–501.

[20] Yizhong Peng XQ, Shu Hongyang, Tian Shuo, Yang Wenbo, Chen Songfeng, Lin Hui, et al. Proper animal experimental designs for preclinical research of biomaterials for intervertebral disc regeneration 2021;2(2):91–142.

[21] Chen D, Xia D, Pan Z, Xu D, Zhou Y, Wu Y, et al. Metformin protects against apoptosis and senescence in nucleus pulposus cells and ameliorates disc degeneration in vivo. Cell Death Dis 2016;7(10):e2441.

[22] Elliott DM, Yerramalli CS, Beckstein JC, Boxberger JI, Johannessen W, Vresilovic EJ. The effect of relative needle diameter in puncture and sham injection animal models of degeneration. Spine 2008;33(6):588–96.

[23] Han B, Zhu K, Li FC, Xiao YX, Feng J, Shi ZL, et al. A simple disc degeneration model induced by percutaneous needle puncture in the rat tail. Spine 2008;33(18): 1925–34.

[24] Zhu L, Jia S, Liu T, Yan L, Huang D, Wang Z, et al. Aligned PCL fiber conduits immobilized with nerve growth factor gradients enhance and direct sciatic nerve regeneration. Adv Funct Mater 2020;30(39).

[25] Causa F, Manto L, Borzacchiello A, De Santis R, Netti PA, Ambrosio L, et al. Spatial and structural dependence of mechanical properties of porcine intervertebral disc. J Mater Sci Mater Med 2002;13(12):77–80. https://doi.org/10.1023/a: 1021143516436. PMID: 15348677.

[26] Cloyd JM, Malhotra NR, Weng L, Chen W, Mauck RL, Elliott DM. Material properties in unconfined compression of human nucleus pulposus, injectable hyaluronic acid-based hydrogels and tissue engineering scaffolds. Eur Spine J 2007; 16(11):1892–8.

[27] Daza Agudelo JI, Ramirez MR, Henquin ER, Rintoul I. Modelling of swelling of PVA hydrogels considering non-ideal mixing behaviour of PVA and water. J Mater Chem B 2019;7(25):4049–54.

[28] Xu Z, Li J, Zhou H, Jiang X, Yang C, Wang F, et al. Morphological and swelling behavior of cellulose nanofiber (CNF)/poly(vinyl alcohol) (PVA) hydrogels: poly(ethylene glycol) (PEG) as porogen. RSC Adv 2016;6(49):43626–33.

[29] Borenstein D. Mechanical low back pain–a rheumatologist's view. Nat Rev Rheumatol 2013;9(11):643–53.

[30] Chen S, Chen M, Wu X, Lin S, Tao C, Cao H, et al. Global, regional and national burden of low back pain 1990-2019: A systematic analysis of the Global Burden of Disease study 2019. J Orthop Translat 2021;32:49–58. https://doi.org/10.1016/j.jot.2021.07.005.

[31] Zhang YS, Khademhosseini A. Advances in engineering hydrogels. Science 2017; 356.

[32] Newell N, Carpanen D, Evans JH, Pearcy MJ, Masouros SD. Mechanical function of the nucleus pulposus of the intervertebral disc under high rates of loading. Spine 2019;44(15):1035–41.

[33] Park H, Guo X, Temenoff JS, Tabata Y, Caplan AI, Kasper FK, et al. Effect of swelling ratio of injectable hydrogel composites on chondrogenic differentiation of encapsulated rabbit marrow mesenchymal stem cells in vitro. Biomacromolecules 2009;10(3):541–6.

[34] Michel R, Poirier L, van Poelvoorde Q, Legagneux J, Manassero M, Corte L. Interfacial fluid transport is a key to hydrogel bioadhesion. Proc Natl Acad Sci U S A 2019;116(3):738–43.

[35] Gupta S, Webster TJ, Sinha A. Evolution of PVA gels prepared without crosslinking agents as a cell adhesive surface. J Mater Sci Mater Med 2011;22(7):1763–72.

[36] Saggese T, Thambyah A, Wade K, McGlashan SR. Differential response of bovine mature nucleus pulposus and notochordal cells to hydrostatic pressure and glucose restriction. Cartilage 2020;11(2):221–33.

[37] Wang S, Li J, Tian J, Yu Z, Gao K, Shao J, et al. High amplitude and low frequency cyclic mechanical strain promotes degeneration of human nucleus pulposus cells via the NF-kappaB p65 pathway. J Cell Physiol 2018;233(9):7206–16.

[38] Bowles RD, Gebhard HH, Hartl R, Bonassar LJ. Tissue-engineered intervertebral discs produce new matrix, maintain disc height, and restore biomechanical function to the rodent spine. Proc Natl Acad Sci U S A 2011;108(32):13106–11.

[39] Chan SC, Ferguson SJ, Gantenbein-Ritter B. The effects of dynamic loading on the intervertebral disc. Eur Spine J 2011;20(11):1796–812.

[40] Miyamoto H, Doita M, Nishida K, Yamamoto T, Sumi M, Kurosaka M. Effects of cyclic mechanical stress on the production of inflammatory agents by nucleus pulposus and anulus fibrosus derived cells in vitro. Spine 2006;31:4–9.

[41] Wang Q. The cornerstone of translational research - selection of appropriate animal models. Biomaterials Translational 2021;2(2):87–8.

[42] Pandit P, Talbott JF, Pedoia V, Dillon W, Majumdar S. T1rho and T2 -based characterization of regional variations in intervertebral discs to detect early degenerative changes. J Orthop Res 2016;34(8):1373–81.

[43] Zehra U, Robson-Brown K, Adams MA, Dolan P. Porosity and thickness of the vertebral endplate depend on local mechanical loading. Spine 2015;40(15): 1173–80.

[44] Molladavoodi S, McMorran J, Gregory D. Mechanobiology of annulus fibrosus and nucleus pulposus cells in intervertebral discs. Cell Tissue Res 2020;379(3):429–44.

[45] Grolman JM, Weinand P, Mooney DJ. Extracellular matrix plasticity as a driver of cell spreading. Proc Natl Acad Sci U S A 2020;117(42):25999–6007.